J Therm Anal Calorim (2010) 100:975–980
DOI 10.1007/s10973-009-0642-y

Nonisothermal calorimetric study of the precipitation processes in a Cu–1Co–0.5Ti alloy

E. Donoso · A. Zúñiga · M. J. Diánez · J. M. Criado

Received: 28 May 2009 / Accepted: 8 December 2009 / Published online: 13 January 2010

Abstract The precipitation processes in a Cu–1.0 at.% Co–0.5 at.%Ti (Cu–1.5 at.%Co_2Ti) alloy were studied using differential scanning calorimetry (DSC), transmission electron microscopy (TEM), and microhardeness measurements. The analysis of the calorimetric curves from room temperature to 900 K shows the presence of two exothermic reactions attributed to the formation of CoTi and Co_2Ti particles in the copper matrix. On the basis of enthalpy calculations, it was found that the decomposition begins with the precipitation of CoTi, followed by the formation of Co_2Ti particles. The activation energies calculated using the modified Kissinger method were lower than the ones corresponding to diffusion of cobalt and titanium in copper. Kinetic parameters were obtained by a convolution method based on the Johnson–Mehl–Avrami (JMA) formalism. The values obtained for the parameter n were indicative of a particle nucleation process from preexistent nuclei. Microhardness measurements and TEM micrographs confirmed the formation of the mentioned phases.

Keywords Copper alloys · DSC · Kinetics · Precipitation · Cu–Co–Ti alloys

E. Donoso (✉)
Departamento de Ciencia de los Materiales, Facultad de Ciencias Físicas y Matemáticas, Universidad de Chile, Casilla, 2777 Santiago, Chile
e-mail: edonoso@ing.uchile.cl

A. Zúñiga
Departamento de Ingeniería Mecánica, Facultad de Ciencias Físicas y Matemáticas, Universidad de Chile, Casilla, 2777 Santiago, Chile

M. J. Diánez · J. M. Criado
Instituto de Ciencias de Materiales de Sevilla, Américo Vespucio S/N Isla de la Cartuja, Sevilla, Spain

Introduction

The development of novel high-strength ternary alloys has been the subject of a series of studies since the middle of the past decade. A majority of these studies explain such resistance by the formation of extremely fine binary and/or ternary precipitates which are resistant to shear by dislocations, lending the material a high yield stress. Good examples of this effect can be found in Cu–Co–Si [1–4], Cu–Co–Ti [5–7], Cu–Al–Co [8], and Cu–Ni–Al [9–11] alloys.

In the case of the Cu–Co–Ti alloys, the precipitation processes have been studied using X-ray Diffraction (XRD) [12–14], Transmission Electronic Microscopy (TEM), and X-ray Energy Dispersion Spectroscopy (EDS) [5, 6]. These studies indicate that depending upon the concentrations of Co and Ti, spherical CoTi and/or Co_2Ti precipitates with cubic structure may develop, with lattice parameters of 0.299 and 1.129 nm, respectively [13].

On the contrary, the experimental results of Mineau et al. [5] suggest that the solubility limit of the CoTi phase in copper, in the 773–1230 K temperature range, is much lower than the individual solubility of the Ti and the Co in the Cu matrix, resulting in a strong tendency to form CoTi particles in the ternary alloy Cu–Co–Ti alloy instead of particles of Co, Cu_3Ti o Cu_4Ti particles. The kinetic analysis of the precipitation in Cu–Co–Ti alloys of quasi-binary compositions Cu–*x*CoTi with a cobalt and titanium concentration at which only the formation of a CoTi precipitate was allowed was carried out in an article earlier [7].

The main objective of this study is to evaluate both the thermodynamic and kinetics of the precipitation process of CoTi and Co_2Ti particles in a supersaturated Cu–Co–Ti solid solution using Differential Scanning Calorimetry (DSC), TEM, and microhardeness measurements.

Experimental method

The alloy used was prepared in an induction furnace, in an inert atmosphere (Ar), from electrolytic copper (99.95% purity) supplied by MADECO (Chile) and both a master alloy of Cu–10 wt%Co and high-purity titanium supplied by Goodfellow Metals (England). The ingot was annealed at 1173 K during 24 h to achieve complete homogenization and then furnace-cooled to room temperature. After chemical analysis, it was found that the alloy contained the following atomic percentages of the constitutive elements: Cu, 98.45%; Co, 1.03%; and Ti, 0.52% (Cu–1.0 at.% Co–0.5 at.%Ti hereafter). Subsequently, the material was cold-rolled to a thickness of 3 mm with intermediate anneal of 1 h at 1173 K. After the last anneal, the material was water quenched.

Microcalorimetric measurements were performed in a Dupont 2000 Thermal Analyzer, under an argon flow (10^{-4} m^3 min^{-1}) using a high-purity well-annealed copper disk as reference to increase the sensitivity of the measurements. The base line was obtained using annealed copper both as reference and sample material under the same experimental conditions used for recording the corresponding DSC curves. The error estimated for the determination of the reaction enthalpy choosing this base line was not higher than 6% [1, 15]. A set of DSC diagrams was recorded under these conditions at heating rates β of 0.083, 0.17, 0.33, 0.50, and 0.67 Ks^{-1} from room temperature up to 900 K. The samples were maintained at this temperature during 5 min, and then freely cooled down to room temperature. The set of cooling curves recorded was very similar to each other and had a shape very close to an exponential curve. Once room temperature was reached, a second set of DSC curves was recorded for the annealed samples at the same heating rates previously used for recording the corresponding DSC curve of the first set to be used as base line. This base line represents the heat capacity of the alloy as a function of the temperature under the existing thermal conditions. Its value was in agreement with the Kopp–Newmann rule. The resulting traces were later transformed into differential heat capacity versus temperature curves. The remaining heat capacity, ΔC_p, represents the heat associated to the reactions in solid state occurring during the DSC experiment. Thus, the peaks observed in the ΔC_p versus T curve may be characterized by an enthalpy of reaction for each particular event.

The microstructure was characterized using a FEI Tecnai ST F20 transmission electron microscope operating at 200 kV equipped with an EDS energy dispersive system. Foils were thinned by jet polishing in a 30 vol.% HNO_3 and 70% methanol solution at −35 °C and 30 V.

Microhardness measurements were performed in a high accuracy Duramin −1/−2 Struers machine employing a load of 1.96 N during 10 s on specimen disks. Such measurements were made using quenched specimens and subsequently annealed specimens at several temperatures for different times. Each microhardness value was calculated from an average of 10 microhardness indentations, with a standard deviation of approximately 2%.

Results and discussion

Typical DSC curves for quenched alloys recorded at different heating rates are shown in Fig. 1. In the DSC curves, two successive exothermic semi-overlapped peaks (stages 1 and 2) are observed. The stages 1 and 2 can be associated to the formation of CoTi and Co_2Ti particles, respectively [5]. It is noteworthy to point out that the enthalpy associated to the exothermic peaks as calculated from the integration of the overall DSC curves was equal to 214 ± 6 J mol^{-1}, independently of the heating rate used, what means that the precipitate composition after the DSC is not influenced by the heating rate. Moreover, the fact that the peak temperature shifts to higher temperatures by increasing the heating rate shows the kinetic control of the process [15].

The enthalpies, ΔH_1 and ΔH_2, determined by integrating the area enclosed by the DSC curve, separated by a convolution method that will be discussed later on, are shown in Table 1. The ΔH value reported for each heating rate was determined as the average of five DSC experiments, and the corresponding error was been estimated as the standard deviation.

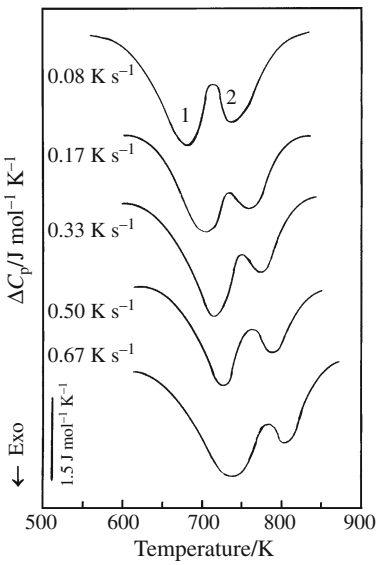

Fig. 1 Calorimetric curves at different heating rates obtained for Cu–1Co–0.5Ti samples previously quenched from 1173 K

The value of the precipitation heat, ΔH_c, of CoTi, calculated as described by us in a previous work [7], was approximately 138 J mol^{-1}, using the molar heat of precipitation ($\Delta H_p = 35.8$ kJ mol^{-1}) in the expression $\Delta H_c = \Delta H_p[c_{CoTi} - c_M(T_f)]$, where c_{CoTi} is the concentration of CoTi in the alloy and $c_M(T_f)$ is the composition of the matrix at the final reaction temperature. The values of c_M were determined from the solubility curves proposed by Mineau et al. [5]. It can be observed that the average value of the experimental reaction heat corresponding to stage 1 (obtained from the DSC curve) is approximately equal to the value previously reported for ΔH_c, which confirms that this stage is due to the formation of CoTi particles, what is in agreement with the XRD and TEM results reported elsewhere [5].

In order to study the precipitation kinetics of the present reactions, effective activation energies E were evaluated from the isoconversional Kissinger equation as modified by Mittemeijer et al. [16], which allows determining the activation energy without any previous assumptions on the kinetic law obeyed by the reaction:

$$\ln\left(\frac{T_p^2}{\beta}\right) = \frac{E}{RT_p} + \ln\left(\frac{E}{RA}\right) \quad (1)$$

where T_p is the peak temperature, A is an Arrhenius pre-exponential factor, and R is the gas constant. Therefore, E and A can be obtained from the plot $ln(T_p^2/\beta)$ versus $1/T_p$, as shown in Fig. 2. In Table 2, one can read the respective values of the activation energy and Arrhenius pre-exponential factor, obtained from this plot. The activation energy for diffusion of Co into Cu ($E_{Co\rightarrow Cu} = 200.6$ kJ mol^{-1}) and Ti in Cu ($E_{Ti\rightarrow Cu} = 200.3$ kJ mol^{-1}) estimated from the Brown and Ashby [17] correlations is much higher than the value calculated from the Kissinger method. This fact can be attributed to the strong contribution of quenching of vacancies, with an activating energy for migration of about one half of the above values.

The kinetic analysis of the reaction was performed according to the Johnson–Mehl–Avrami (JMA) equation, which is usually used for heterogeneous reactions under nonisothermal conditions. According to this kinetic model, the reaction rate can be expressed by the following equation.

Table 1 Reaction enthalpies from a set of DSC curves recorded at different heating rates starting from Cu-1.5% Co_2Ti samples previously quenched from 1173 K

β/K s^{-1}	0.08	0.17	0.33	0.50	0.67
ΔH_1/J mol^{-1}	134 ± 7	128 ± 6	136 ± 7	125 ± 6	140 ± 7
ΔH_2/J mol^{-1}	101 ± 5	83 ± 5	71 ± 4	75 ± 4	78 ± 4

Data represent the average of five DSC runs

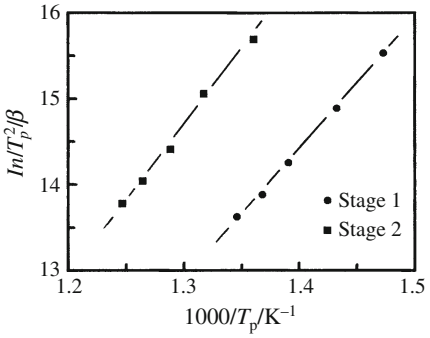

Fig. 2 Modified Kissinger plot for evaluating the activation energy and pre-exponential factor

Table 2 Values of activation energies and Arrhenius pre-exponential factors

	E/kJ mol^{-1}	ln A; A/s^{-1}
Stage 1	126 ± 3	16.5 ± 0.2
Stage 2	143 ± 4	17.5 ± 0.2

$$\frac{d\alpha}{dt} = Ae^{-E/RT}\, n(1-\alpha)\left[-\ln(1-\alpha)^{1-\frac{1}{n}}\right] \quad (2)$$

where α is the reacted fraction, n is a constant that depends on the reaction model, t is the reaction time, and A is the Arrhenius pre-exponential factor.

If the reaction is carried out at a constant temperature, the integration of Eq. 2 leads to:

$$[-\ln(1-\alpha)]^{1/n} = kt \quad (3)$$

where $k = A\ e^{-E/RT}$ accounts for the constant rate at the temperature T.

However, if the reaction is conducted under a linear heating rate $\beta = dT/dt$, the integration of Eq. 3 using the Coats and Redfern approach [18] gives:

$$[-\ln(1-\alpha)]^{1/n} = \frac{ART^2}{\beta E}e^{-E/RT} \quad (4)$$

which can be represented in logarithmic form in the following way.

$$\ln[-\ln(1-\alpha)] = n\ln A + n\ln\left[\frac{RT^2}{\beta E}\exp(-E/RT)\right] \quad (5)$$

The term $\theta = RT^2/\beta E\ \exp(-E/RT)$ represents the reduced time introduced by Ozawa [19]. The use of θ for obtaining normalized master plots that can be indistinctly used for the kinetic analysis of isothermal and nonisothermal data was described in a previous reference [15].

If two DSC peaks overlap each other, such is the situation for stage 1 and 2, the total heat flow $\Delta \dot{H}_T$ per unit mass at any time/temperature can be expressed as the sum of the heat flow of the individual transformation $\Delta \dot{H}_1$ and $\Delta \dot{H}_2$ as [3, 20, 21]:

$$\Delta \dot{H}_T = \Delta \dot{H}_1 + \Delta \dot{H}_2 = S_1 \dot{\alpha}_1 + S_2 \dot{\alpha}_2 \tag{6}$$

where S_1 and S_2 are the areas of the individual peaks, while $\dot{\alpha}_1$ and $\dot{\alpha}_2$ are the transformation rates, being easily derived for each reaction.

And, with the aid of Eq. 5 becomes [3, 20, 21]:

$$\dot{\alpha} = nA^n \left(\frac{T^2 R}{\beta E}\right)^{n-1} \exp\left(-\frac{nE}{RT}\right) \exp\left[-A^n \left(\frac{T^2 R}{\beta E}\right)^n \exp\left(-\frac{nE}{RT}\right)\right] \tag{7}$$

From Eq. 6, after assigning to reactions 1 and 2 the respective subscripts, the following equation is obtained.

$$\dot{H}_T = \sum_{i=1}^{2} S_i n_i A_i^n \left(\frac{T^2 R}{\beta E_i}\right)^{n_i - 1} \exp\left(-\frac{n_i E_i}{RT}\right) \exp\left\{-\left[\left(\frac{T^2 R}{\beta E_i}\right)^{n_i} A \exp\left(-\frac{n_i E_i}{RT}\right)\right]\right\} \tag{8}$$

The area of the individual peaks must add up the total area $S = S_1 + S_2$. By fitting this equation to the experimental heat flow data $\Delta \dot{H}_T$ employing computerized methods of minimization of least-squares error method, the parameters $n_1 = 1.15$ and $n_2 = 1.52$ can be obtained, which in conjunction with the effective activation energies E_1 and E_2 and the pre-exponential factors of Arrhenius calculated from the modified Kissinger method constitute the kinetic parameters for each individual reaction. Also, the parameters S_1 and S_2 can be calculated and since the heat flow per unit mass of the sample $\Delta \dot{H} = \Delta C_p \beta / MW_S$ where MW_S (=63.426 $\times$ 10^{-3} kg mol^{-1}) is the molecular mass of the precipitate, the associated reaction heat can be, therefore, readily obtained. The respective average values obtained are $\Delta H_1 = 133$ J mol^{-1} and $\Delta H_2 = 82$ J mol^{-1}. The DSC curves included in Fig. 1 have been reconstructed by means of Eq. 8 after substituting the values determined for the kinetic parameters. The matching of the reconstructed curve with the experimental DSC curve obtained at 0.17 Ks^{-1} shown in Fig. 3 by way of example supports the validity of the computation method used. Moreover, the value of n_1 here obtained is closely indicative of a nucleation and growth controlled process, while that for n_2 supports a growth process from pre-existing nuclei of nonnegligible size [22].

The microstructures of the CoTi and Co_2Ti phases were studied by means of TEM, and Energy Dispersive X-ray

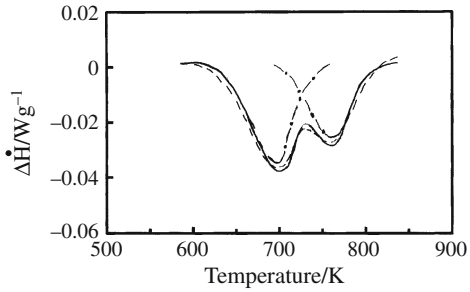

Fig. 3 Heat flow against temperature from DSC experiments at $\beta = 0.17$ Ks^{-1}. (*solid line*) Experimental composite curve; (*dashed line*) calculated composite curve; (*dashed dotted line*) approximation to individual stages 1 and 2

Spectroscopy, EDS. Figure 4 shows a TEM image and microanalysis (EDS) performed on the fine precipitates formed in the Cu–1Co–0.5Ti alloy after quenching and after aging at 673 K for 12.6 ks. The TEM/EDS microanalyses give a Co/Ti ratio of about 1.1 in particles with an average size of approximately 150 nm, which might correspond to the CoTi precipitates. No Co or Ti particles were observed since the solubility limit of the CoTi phase in copper is much lower than the individual solubility of Co and Ti, as shown in Fig. 5 of the Mineau et al. report [5]. The strong tendency to form CoTi in the ternary Cu–Co–Ti alloy is consistent with the low solubility in copper. Figure 5 shows a TEM image and EDS microanalysis

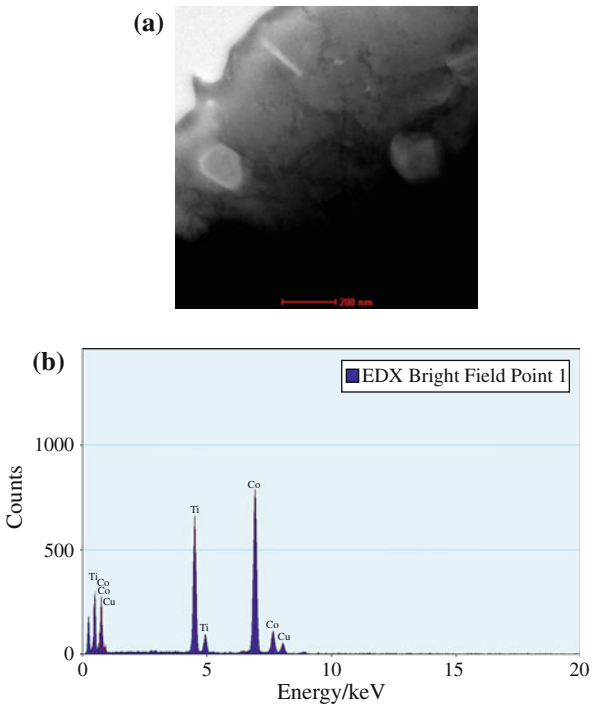

Fig. 4 STEM image and microanalysis (EDS) of a Cu–1Co–0.5Ti alloy after heat treatment at 673 K for 12.6 ks

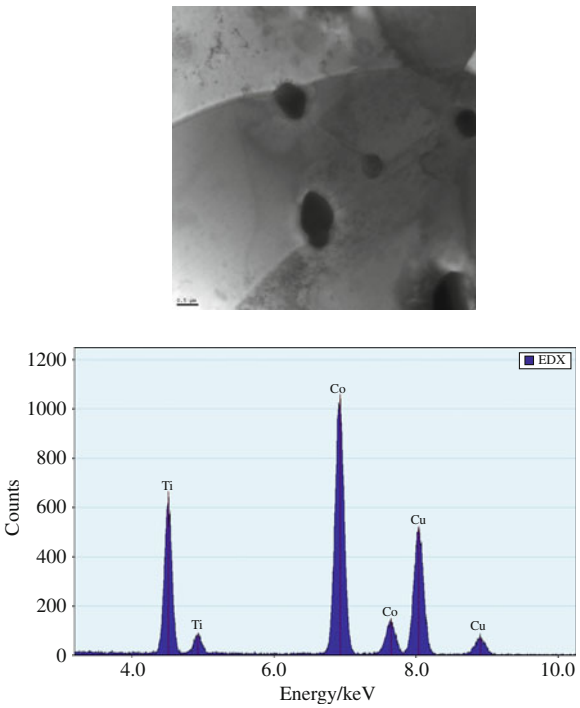

Fig. 5 TEM images and microanalysis (EDS) of a Cu–1Co–0.5Ti alloy after heat treatment at 800 K for 14.4 ks

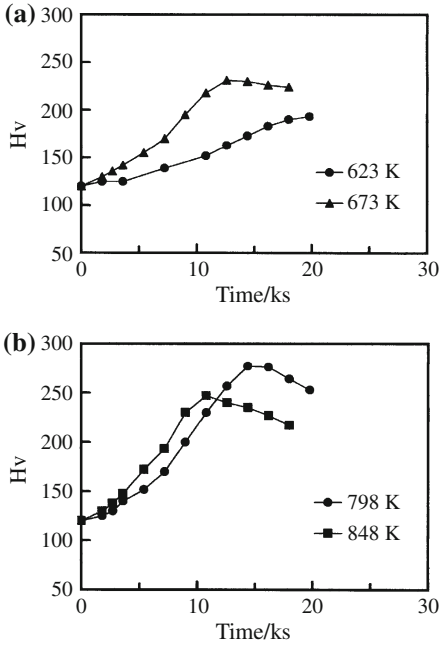

Fig. 6 Vickers microhardness versus time for different aging temperatures (samples previously quenched from 1173 K) measured under a load of 1.96 N

performed on the small particles formed in the alloy after quenching and after aging at 800 K for 14.4 ks. TEM observations show that the alloy consists of fine spherical precipitates with a mean diameter of about 700 nm. In this case, the Co/Ti ratio is closer to the stoichiometry 2/1, which corresponds to the Co_2Ti intermetallic phase. In summary, the TEM micrographs and microanalysis, along with the DSC results, indicate that the precipitation process starts with the formation of CoTi followed by Co_2Ti precipitate formation.

In addition, isothermal Vickers microhardness measurements in quenched material with annealing treatments at several temperatures were made. Figure 6a shows the variation of hardness versus time at 623 and 673 K. It can be observed that the Vickers hardness increase with time until a maximum value is reached, for the annealing temperature of 673 K. In the case of aging at 623 K, it is possible that the reaction is not completed at the aging times explored in this investigation. The aging curves at 800 and 850 K are shown in Fig. 6b. It can be observed that the hardness value increases with time until a maximum value is reached, for both annealing temperatures (800 and 850 K). These maximum values indicate that an equilibrium precipitation degree is attained in each case. A peak hardness of 277 Hv is observed after aging at 800 K for 14.4 ks, beyond which it decreased with aging time. At 850 K, the peak hardness is found to be slightly lower (247 Hv for 10.8 ks). The decrease of the hardness after annealing at 850 °C would be attributed to the growing of the Co_2Ti crystal formed. On the contrary, it would be noteworthy to remark that the formation of Co_2Ti precipitates leads to a higher alloy hardness than the Co_2Ti precipitates despite that their size is larger than the corresponding one to the CoTi formed at lower temperatures. Thus, the development of preparation of Cu–Ti–Co alloys, which allows to decrease the crystal size of the Co_2Ti precipitates, would be of great interest for improving the mechanical properties of these alloys.

Conclusions

The foregoing results allow us to draw the following conclusions: (a) the calorimetric curves indicate that the precipitation process evolves in two stages, which correspond to the formation of CoTi and Co_2Ti particles, respectively, (b) the activation energies resulted be lower than those corresponding to the diffusion of cobalt in copper and titanium in copper, which can be explained due to the contribution of vacancies introduced during quenching, (c) the value obtained for the constant n suggests that the formation of the CoTi phase occurs through a nucleation and growth controlled process starting from a solid solution, followed by the formation of Co_2Ti precipitate, (d) TEM and EDS analyses suggest that the formation of CoTi followed by its conversion into Co_2Ti phase takes place, and (f) microhardness measurements confirm that the increase of the

hardness of the alloy is associated to the formation of CoTi and Co_2Ti particles.

Acknowledgements The authors would like to acknowledge the Fondo Nacional de Desarrollo Científico y Tecnológico (FONDECYT) for the financial support, Project No. 1090010. The access to specialized facilities and laboratories provided by the Instituto de Ciencias de Materiales de Sevilla, Spain and the Departamento de Ciencia de los Materiales, Facultad de Ciencias Físicas y Matemáticas, Universidad de Chile is also greatly appreciated.

References

1. Varschavsky A, Donoso E. Energetic and kinetic evaluations conducted in a quasi-binary Cu-1at.%Co_2Si alloy through DSC. J Thermal Anal Cal. 2002;68:231–41.
2. Donoso E. Calorimetric evaluation of precipitation in Cu rich, Cu-Co-Si. Rev Metal Madrid. 2001;37:492–8.
3. Varchavsky A, Donoso E. DSC study of precipitation processes in Cu-Co-Si alloys. J Thermal Anal Cal. 2003;74:41–56.
4. Albert B. Löslichkeit und ausscheidungsvorgänge in Cu-Co-Si-Legierungen. Z Metallkde. 1985;76:475–8.
5. Mineau L, Hamar-Thibault S, Allibert CH. Precipitation in Cu-rich Co-Ti ternary alloys. Phys Stat Sol A. 1992;134:93–105.
6. Batra IS, Laik A, Kale GB, Dey GK, Kulkarni UD. Microstructure and properties of a Cu-Ti-Co alloy. Mater Sci Eng A. 2005;402:118–25.
7. Donoso E, Diaz G, Criado JM. Kinetics analysis of precipitation in a quasi-binary Cu-1at.% CoTi alloy. J Thermal Anal Cal. 2008;91:491–5.
8. Fortina G, Leoni M. Caratteristiche strutturali, meccaniche e di resistenza alla corrosion di nuovi tipi di bronzo di alluminio al cobalto. Metal Italiana. 1972;10:470–80.
9. Sierpinski Z, Gryziecki J. Phase transformations and strengthening during ageing of CuNi10Al3 alloy. Mater Sci Eng A. 1999;264:279–85.
10. Sierpinski Z, Gryziecki J. Precipitation and recrystallization processes during ageing of plastically deformed Cu-6wt%Ni-3wt%Al. Z Metallkd. 1998;89:551–3.
11. Donoso E, Diánez MJ, Sayagués MJ, Criado JM, Varschavsky A, Díaz G. Non isothermal calorimetric study of the precipitation processes in a Cu-10%Ni-3%Al alloy. Rev Metal Madrid. 2007;43:117–24.
12. Pfeifer HU, Bhan S, Schubert K. Zum aufbau des systems Ti—Ni—Cu und einiger quasihomologer legierungen. J Less-common Met. 1968;14:291–302.
13. Murray JL. The Al-Mg (Aluminium-Magnesium) system. Bull Alloy Phase Diagr. 1982;3:74–85.
14. Gupta KP. The Co-Cu-Ti (cobalt-copper-titanium) system. J Phase Equil. 2003;24:272–5.
15. Gotor FJ, Criado JM, Málek J, Koga N. Kinetic analysis of solid-state reactions: the universality of master plots for analyzing isothermal and nonisothermal experiments. J Phys Chem A. 2000;104:10777–82.
16. Mittemeijer EJ, Cheng L, Van der Shaaf PJ, Brakman CM, Korevaar BM. Analysis of nonisothermal transformation kinetics; tempering of iron-carbon and iron-nitrogen martensites. Metall Trans A. 1988;19:925–32.
17. Brown AM, Ashby MF. Correlations for diffusion constants. Acta Metall. 1980;28:1085–101.
18. Coats AW, Redfern JP. Kinetic parameters from thermogravimetric data. Nature 1964;201:68–9.
19. Ozawa T. A modified method for kinetic analysis of thermoanalytical data. J Thermal Anal. 1976;9:369–73.
20. Borrego A, González-Doncel G. Calorimetric study of 6061-Al-15vol.%SiC_w PM composites extruded at different temperatures. Mater Sci Eng A. 1998;245:10–8.
21. Borrego A, González-Doncel G. Reply to comments on: calorimetric study of 6061-Al-15vol.%SiC_w PM composites extruded at different temperatures. Mater Sci Eng A. 2000;276:292–5.
22. Christian JW. The theory of transformation of metals and alloys. 2nd ed ed. England: Pergamon Press; 1971. p. 534.